Vortex lattices in the lowest Landau level for confined Bose-Einstein condensates

N.R. Cooper, S. Komineas
Theory of Condensed Matter Group, Cavendish Laboratory, Madingley Road, Cambridge CB3 0HE, United Kingdom

N. Read
Department of Physics, Yale University, P.O. Box 208120, New Haven, CT 06520-8120.

(Dated: February 2, 2008)

We present the results of numerical calculations of the groundstates of weakly-interacting Bose-Einstein condensates containing large numbers of vortices. Our calculations show that these groundstates appear to be close to uniform triangular vortex lattices. However, slight deviations from a uniform triangular lattice have dramatic consequences on the overall particle distribution. In particular, we demonstrate that the overall particle distribution averaged on a lengthscale large compared to the vortex lattice constant is well approximated by a Thomas-Fermi profile.

PACS numbers: 03.75.Kk, 05.30.Jp

I. INTRODUCTION

Experiments on rotating Bose condensates at high angular momentum have reached the limit in which the vortex cores overlap strongly [1]. In this limit, the single particle states are restricted to states in the lowest Landau level (LLL) [2, 3]. The vortices cannot be considered to interact by pairwise interactions, but have intrinsically multi-vortex interactions [4], leading to a very interesting regime of vortex physics.

In an influential theoretical paper studying the nature of the vortex lattices in this regime [5], the assumption was made that the vortices will form a uniform triangular lattice. Under this assumption, it was shown that the particle density averaged over a lengthscale large compared to the intervortex spacing has a Gaussian profile. One can, however, expect that in the true LLL groundstate the vortices will not form an ideal triangular lattice, and that small changes in vortex position could lead to a rather different overall density profile; within simple approximate considerations, when there are a large number of vortices one would expect these deviations to lead to a Thomas-Fermi profile for the average particle distribution [6, 7, 8], which for a harmonic trap is an inverted parabola as a function of the distance from the rotation axis.

We expect that the LLL approximation is an excellent guide to the low-energy properties (including the ground state density profile) whenever the ratio, λ, of the interaction energy scale to the level spacing of the transverse harmonic confinement in an axially symmetric trap, $\lambda \equiv 4\pi\hbar^2 a_s \bar{n}/(M\hbar\omega_\perp)$, is much smaller than unity ($\bar{n}$ is the typical number density of bosons, a_s the s-wave scattering length, M the particle mass, and $\omega_\perp$ is the trapping frequency perpendicular to the rotation axis). We term $\lambda \ll 1$ the LLL regime. Note that the condition for being in this regime does not involve the system size. When many vortices are present, it is equivalent to the healing length being larger than the vortex spacing. There will be perturbative corrections to the LLL approximation, in powers of the interaction parameter λ. An earlier work [8, 9], which extends into the LLL regime, finds within a variational ansatz that even if one neglects the deformations of the vortex lattice that we study here, a TF profile emerges through weak Landau level mixing provided the healing length is small compared to the sample size. Also Ref. [10] provides a treatment of the averaged density profile in the vortex lattice in the opposite limit in which the healing length is small compared to the vortex spacing, and deviations of the vortex lattice from uniform triangular were found there.

In this paper, we provide explicit numerical calculations of the groundstates of large numbers of vortices in atomic Bose condensates in the LLL limit. By comparing our full variational results for the many-vortex groundstate with the results obtained under the assumption of a uniform triangular vortex lattice, we show that the small changes in the vortex position in the true groundstate away from a uniform lattice have a dramatic effect on the overall density profile. In particular, we demonstrate that the coarse-grained particle density of a system containing a large number of vortices is well approximated by a Thomas-Fermi profile. The accuracy of the Thomas-Fermi profile in describing this regime can already be seen from the results of the numerical studies of Sinova *et al.* [7] where the coarse-grained particle density for a small vortex lattice array in the LLL was found to fit an inverted parabola.

II. MODEL

We consider the rotating Bose gas when interactions are sufficiently weak to enter the LLL regime ($\lambda \ll 1$) and, furthermore, to allow restriction to the two-dimensional (2D) limit in which all particles occupy the lowest harmonic oscillator state of the axial confinement (accurate provided $4\pi\hbar^2 a_s \bar{n}/(M\hbar\omega_\parallel) \ll 1$, where $\omega_\parallel$ is the trapping frequency parallel to the rotation axis). Although these conditions are far from being satisfied in

atomic gases in the absence of rotation, at high angular momentum the radial expansion of the cloud due to the centrifugal forces reduces the mean particle density and leads the system towards the weakly-interacting limit [5, 9]. Indeed, recent experiments [1] have reached conditions that are within the LLL regime and close to the 2D limit.

In this paper we shall restrict attention to the case where the filling fraction (the ratio of the number of particles to the number of vortices [11]) is sufficiently large that the groundstate is a vortex lattice [11, 12] and can be well-described by Gross-Pitaevskii theory. In the case of interest – weak contact interactions – Gross-Pitaevksii theory for the groundstate amounts to minimizing the interaction energy

$$E_{\rm int} = \frac{2\pi\hbar^2 a_s N^2}{M}\int |\psi(\boldsymbol{r})|^4\, d^3\boldsymbol{r} \tag{1}$$

within the space of states in the lowest subband of the axial confinement (z) and in the lowest Landau level of the transverse ($x-y$) motion. Such states may be written

$$\psi(\boldsymbol{r}) = A\prod_j (\eta-\eta_j) e^{-|\eta|^2/(2a_\perp^2)} e^{-z^2/(2a_\parallel^2)} \tag{2}$$

where $\eta=(x+iy)$, and $a_{\parallel,\perp}\equiv\sqrt{\frac{\hbar}{M\omega_{\parallel,\perp}}}$ are the oscillator lengths parallel and perpendicular to the rotation axis. We choose the normalization constant A such that

$$\int |\psi(\boldsymbol{r})|^2 d^3\boldsymbol{r} = 1\,, \tag{3}$$

which is why the number of particles N enters in the expression for the interaction energy, Eqn.(1). The variables η_j are the complex numbers representing the positions of the vortices in the $x-y$ plane. Hence, the wave function (including therefore the particle density) is fully specified by the positions of the vortices. The task is to find the positions of the vortices that minimise the interaction integral as a function of the total angular momentum per particle in units of $\hbar$,

$$\ell = \int d^3\boldsymbol{r}\,\left[-i\psi^*\,\boldsymbol{r}\times\frac{\partial\psi}{\partial\boldsymbol{r}}\cdot\hat{\boldsymbol{z}}\right]. \tag{4}$$

Note that, within the LLL states, the combined kinetic and potential energy (relative to the zero point energy) is proportional to the angular momentum, which is why these energies need not be included explicitly in the minimization when angular momentum is constrained.

The connection between vortex positions and particle density lies at the heart of the difficulty of an exact derivation of the density profile. Variations in the coarse-grained 2D density profile, $\bar{n}_{\rm 2d}(x,y)$, (the particle density $|\psi(\boldsymbol{r})|^2$ averaged over lengthscales large compared to the vortex lattice constant and integrated over the z direction) are by necessity tied to variations in the vortex positions. (A similar relation of superfluid density [which is the same as particle density in the Gross-Pitaevskii theory] and vortex density as in the LLL approximation [5] was found in Ref. [10].) If one makes the assumption that the vortices are only slightly perturbed from a triangular lattice, and ignores the variation of the lattice geometry in the energetics, then one is led to the expectation that the coarse-grained density profile will be an inverted parabola – *i.e.* Thomas-Fermi like [8]. By imposing the normalisation condition (3), and noting that for states in the lowest Landau level, the angular momentum per particle is directly related to the density profile via

$$\ell = \int dxdy\left[\frac{(x^2+y^2)}{a_\perp^2}-1\right]\bar{n}_{2d}(x,y) \tag{5}$$

we find that the Thomas-Fermi profile may be written

$$\bar{n}_{\rm 2d}(\rho) = \frac{2}{3\pi(\ell+1)a_\perp^2}\left[1-\frac{\rho^2}{3(\ell+1)a_\perp^2}\right] \tag{6}$$

where $\rho\equiv\sqrt{x^2+y^2}$. Thus, the radius of the cloud, R, increases with angular momentum per particle as

$$R = \sqrt{3(\ell+1)}\,a_\perp\,. \tag{7}$$

One can also relate the radius to the angular rotation frequency Ω at which the state with angular momentum ℓ is stable. Following the approach of Ref. [8] one finds

$$R = \left[\frac{2bg_{\rm 2D}a_\perp^2}{\pi\hbar(\omega_\perp-\Omega)}\right]^{1/4}, \tag{8}$$

where $b=1.1596$ is the Abrikosov parameter for the energy of a uniform triangular vortex lattice [13] and $g_{\rm 2D}=2\sqrt{2\pi}N\hbar^2 a_s/(a_\parallel M)$.

On the other hand, if one assumes that the vortices form a uniform triangular lattice, then the coarse-grained 2D density profile is of the form [5]:

$$\bar{n}_{\rm 2d}(\rho) = \frac{1}{\pi\sigma^2}e^{-\rho^2/\sigma^2} \tag{9}$$

$$\frac{1}{\sigma^2} = \frac{1}{a_\perp^2}-\pi n_V \tag{10}$$

where n_V is the areal density of vortices. (For a triangular lattice of lattice constant a, the vortex density is $n_V=2/(\sqrt{3}a^2)$.) Using (5), one finds

$$\frac{1}{\sigma^2} = \frac{1}{a_\perp^2}\frac{1}{\ell+1}\,. \tag{11}$$

For the full variational study, a numerical conjugate gradient method is used to minimise the interaction energy (1) with respect to the vortex positions in (2) and subject to the normalisation (3) for a range of values of the fixed angular momentum per particle (4). To this end, it is helpful to expand the wavefunction (2) in terms of the single-particle states in the LLL with angular momentum quantum number m, and write the (normalised) wavefunction in the $x-y$ plane as

$$\phi(\eta) = \sum_{m\geq 0} c_m \frac{\eta^m}{\sqrt{\pi m!}\,a_\perp^{m+1}} e^{-|\eta|^2/(2a_\perp^2)}\,. \tag{12}$$

Constraints on angular momentum per particle and normalisation are then imposed by Lagrange multipliers (in terms of physical parameters these are $\hbar(\omega_\perp - \Omega)N$ and μN, where μ is the chemical potential relative to the zero-point energy). In this way, the variational equations can be expressed in terms of coupled equations for the complex coefficients c_m.

As an aside, we note that the resulting variational equations can be expressed in real-space form as

$$g_{2\mathrm{D}} \int d^2\eta' \delta(\eta,\eta')|\phi(\eta')|^2\phi(\eta') - \mu\phi(\eta) + \hbar(\omega_\perp - \Omega)\int d^2\eta' \delta(\eta,\eta')\frac{\eta\bar{\eta}'}{a_\perp^2}\phi(\eta') \;=\; 0 \quad (13)$$

where

$$\delta(\eta,\eta') = \frac{1}{\pi a_\perp^2}\, e^{\left(-|\eta|^2/2a_\perp^2 - |\eta'|^2/2a_\perp^2 + \eta\bar{\eta}'/a_\perp^2\right)} \qquad (14)$$

is (the integral kernel of) the projection operator to the LLL [14]. Notice that $|\delta(\eta,\eta')|^2 = e^{-|\eta-\eta'|^2/a_\perp^2}/(\pi a_\perp^2)^2$ falls rapidly for $|\eta - \eta'| > a_\perp$. This real-space form of the lowest Landau level variational equations is a useful starting point for further analytic approximations.

Here we focus on the numerical solution to the problem. In our numerical procedure we work in terms of the coefficients c_m, which we allow to be non-zero up to some maximum angular momentum (≤ 300) which we check is sufficiently large to have no significant effect on the results (this is equivalent to setting a maximum number of vortices in (2)). This procedure is identical to that followed in Ref. [3]; the difference is that here we are interested in much larger values of the angular momentum per particle than the cases studied in Ref. [3]. (For the Thomas-Fermi profile, at large angular momentum, one expects the number of visible vortices, N_V, to increase with the angular momentum per particle as $N_V = 3\ell$.)

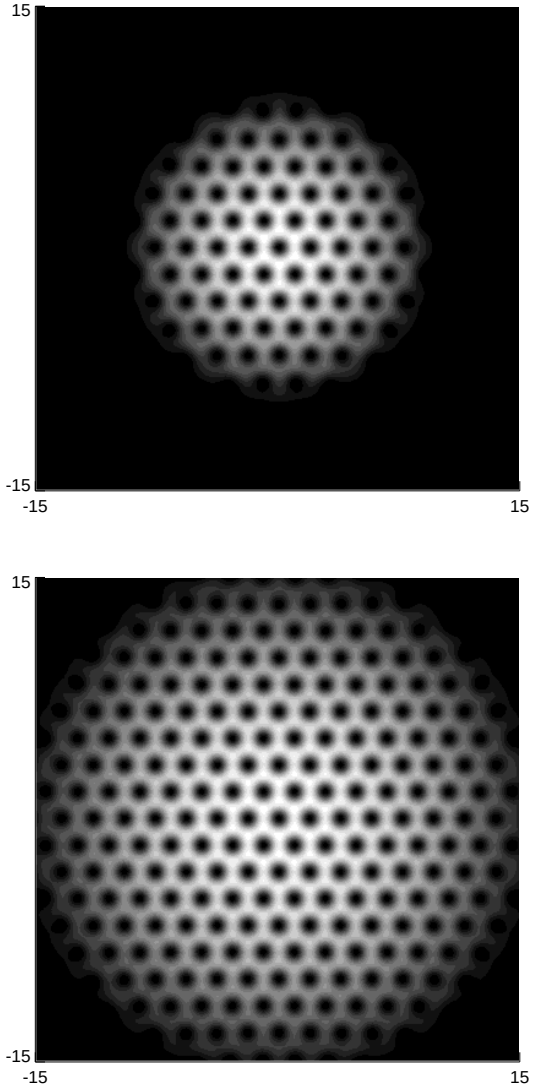

FIG. 1: The particle density for two vortex lattices which are calculated as the minimum of the interaction energy (1). In the upper entry we have angular momentum $\ell = 31$ and in the lower entry $\ell = 91$. The grey-scale code is set to black for vanishing particle density and to white for maximum density which occurs at the central region of the trap.

III. RESULTS

The results of our full variational calculation always show a (slightly distorted) vortex lattice. We focus attention on the case of large angular momentum where the lattice spacing appears to be roughly uniform in the central region of the condensate. For the range of angular momentum that we study, we find that there are stable low-energy configurations of the system in which one vortex is close to the centre of the trap, and around which there is an approximate 6-fold rotation symmetry. One can then choose one of the lines of reflection symmetry to be the x axis. We have tested that such configurations are stable to small deviations around the minimising values, and that they give the lowest energy that we could obtain.

In Fig. 1 we show shadow plots of the particle density for two examples of the results of the full variational study, at $\ell = 31$ and $\ell = 91$. Even though the vortex positions of the full variational groundstate appear to be very close to the positions of a triangular lattice, there are slight deviations from this regular arrangement, especially close to the edge of the cloud. These deviations are sufficient to give a very different overall density profile to that expected from a uniform vortex lattice.

To illustrate this, we have constructed the wavefunctions for the ansatz in which the vortices are at the sites of a uniform triangular lattice [5]. To most closely reproduce our full variational results we choose to position the lattice such that there is a lattice site at the centre of the condensate and there is reflection symmetry in the x-axis. The only remaining freedom in the ansatz is then the value of the lattice constant, which controls the angular momentum per particle.

In Fig. 2 we show the particle densities for this triangular lattice ansatz, with lattice constant chosen to give

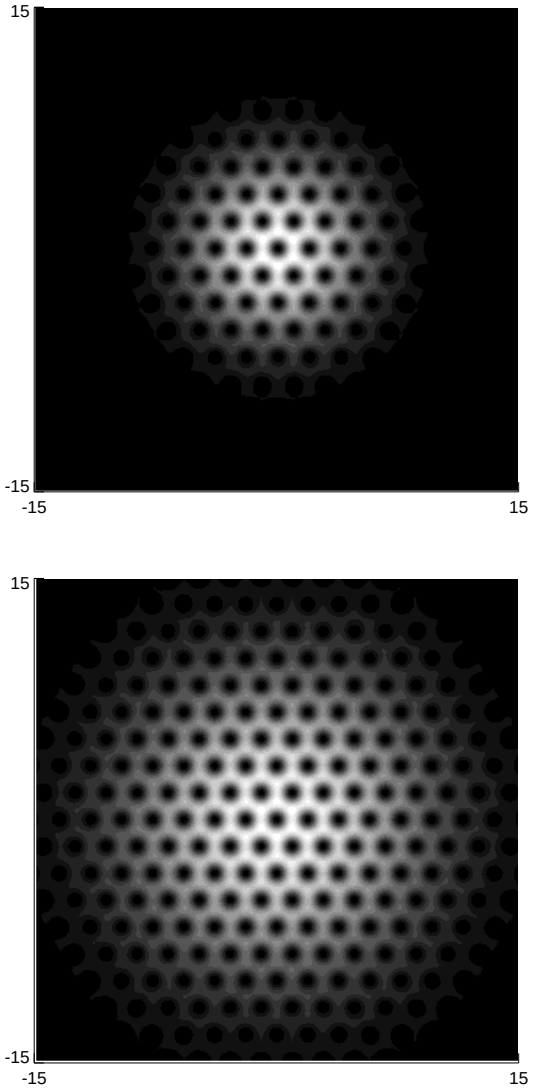

FIG. 2: The particle density for two wavefunctions obtained under the assumpion of a perfect triangular vortex lattice. In the upper entry we use a lattice constant $a = 1.9351a_\perp$ which corresponds to angular momentum $\ell = 31$ and in the lower entry we have $a = 1.9151a_\perp$ which gives $\ell = 91$. The grey-scale code is set to black for vanishing particle density and to white for maximum density which occurs at the central region of the trap. A qualitative comparison with Fig. 1 is easy but note that the white colour in Fig. 1 does not correspond to the same value in the present figure.

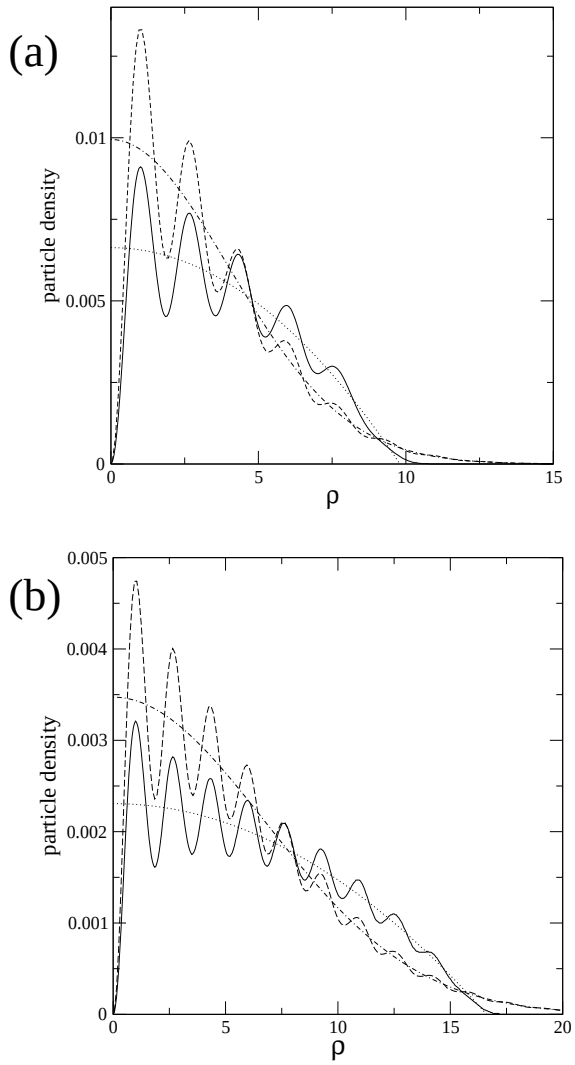

FIG. 3: The angular-averaged particle density as a function of the radial co-ordinate for (a) $\ell = 31$ and (b) $\ell = 91$. (The particle density is in units of $a_\perp^{-2}$ and ρ in units of $a_\perp$.) In both figures, the solid line corresponds to the full variational result, and the dashed line corresponds to the triangular lattice ansatz. The dotted lines are the Thomas-Fermi profiles, Eqn. (6), for (a) $\ell = 31$ and (b) $\ell = 91$, while the dot-dashed curves are the Gaussian profiles (9) for the lattice constant (a) $a = 1.9351a_\perp$, and (b) $a = 1.9151a_\perp$.

angular momenta $\ell = 31$ and $\ell = 91$. The differences between the particle densities obtained from the full variational calculation and from the triangular lattice ansatz are large enough to be seen directly from the shadow plots. The particle density for the triangular ansatz is more peaked at the centre and has a somewhat longer tail at large distances.

To make a more quantitative comparison of the above lattices we have determined the angular-averaged particle density as a function of the radial distance ρ from the trap centre, by writing $\eta = \rho e^{i\varphi}$ and averaging the particle density over the azimuthal variable φ. The results are presented in Figs. 3(a) and (b). The difference between the full variational result and the triangular lattice is very clear for $\ell = 31$ as well as for $\ell = 91$. For both values of angular momentum, the average density profile for the full variational result is very well reproduced by the Thomas-Fermi profile, Eqn. (6) (ignoring the rapid oscillations on the lengthscale of the intervortex spacing). On the other hand, the average particle density for the triangular lattice ansatz is well reproduced by the Gaussian formula (9), consistent with the result of Ref. [5]. The Gaussian and Thomas-Fermi profiles are sufficiently different that it can be clearly seen that the Thomas-Fermi profile provides a significantly better fit to the full variational groundstate than does the Gaussian.

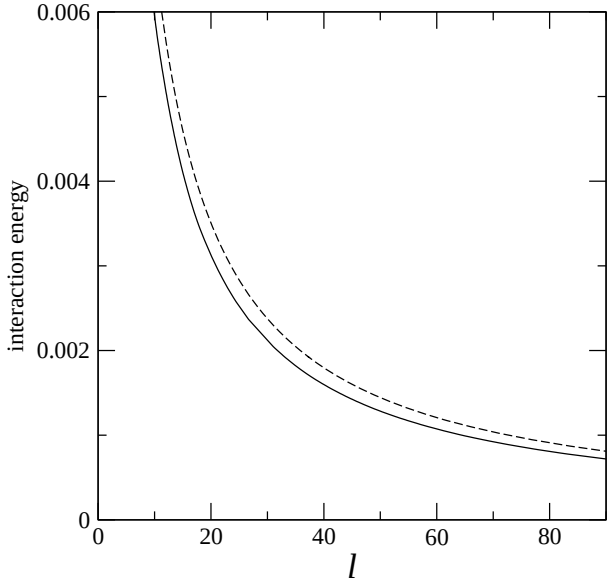

FIG. 4: The interaction energy (1) as a function of the angular momentum per particle, for the full variational groundstate (solid line) and for the triangular lattice ansatz (dashed line). [The interaction energy is plotted in units of $2\pi\hbar^2 a_s N^2/(M a_\perp^2 a_\parallel)$.]

Finally, in Fig. 4 we compare the interaction energies per particle for the full variational wavefunction and the triangular lattice cases as a function of angular momentum per particle. As is required for consistency, the full variational wavefunction has an interaction energy lower than that of the triangular lattice ansatz (by about 10%). The interaction energy for the full variational wavefunction is very closely given by the expression $E_{\rm int}^{\rm var} = 2bg_{2D}N/[9\pi a_\perp^2(\ell+1)]$, which can be found by use of the Thomas-Fermi analysis of Ref. [8]; the corresponding energy for the triangular lattice is $E_{\rm int}^{\rm tri} = bg_{2D}N/[4\pi a_\perp^2(\ell+1)]$. This energy reduction by a factor of 8/9 at fixed angular momentum, ℓ, is equivalent to the energy reduction by a factor of $2\sqrt{2}/3$ at fixed angular frequency Ω found in Ref. [8].

IV. CONCLUSIONS

In conclusion, we have presented the results of numerical calculations of the finite-size vortex lattices in atomic Bose condensates at large values of the angular momentum. We have studied the weakly-interacting limit where vortex cores overlap strongly, and the particles are restricted to states in the lowest Landau level. Our results show clearly that the density distribution of particles averaged over a lengthscale larger than the vortex lattice is very accurately given by a Thomas-Fermi profile. These results indicate that, in the lowest Landau level limit, a fit of the overall density profile found in experiment to a Thomas-Fermi profile, Eqn.(6), can be used as a measure of the angular momentum per particle. Images of the groundstate density profile and vortex locations can be obtained reliably from the expanded cloud (following release of the trapping potential), since for states in the lowest Landau level the wavefunction of the final (expanded) state is directly related to the initial (unexpanded) up to a rescaling and rotation [15].

While preparing this work for publication, we became aware of related numerical studies where similar conclusions were reached [16].

Acknowledgements: We are grateful to C. Pethick, L. Radzihovsky and J. Sinova for helpful correspondence. This work was supported by EPSRC grant nos. GR/R99027/01 (NRC), GR/R96026/01 (SK) and NSF grant no. DMR-02-42949 (NR).

[1] V. Schweikhard, I. Coddington, P. Engels, V.P. Mogendorff, and E.A. Cornell, Phys. Rev. Lett. **92**, 040404 (2004).
[2] N.K. Wilkin, J.M.F. Gunn, and R.A. Smith, Phys. Rev. Lett. **80**, 2265 (1998).
[3] D.A. Butts and D.S. Rokhsar, Nature (London) **397**, 327 (1999).
[4] Z. Tesanovic and L. Xing, Phys. Rev. Lett. **67**, 2729 (1991).
[5] T.-L. Ho, Phys. Rev. Lett. **87**, 060403 (2001).
[6] A. H. MacDonald (private communication).
[7] J. Sinova, C.B. Hanna, and A.H. MacDonald, Phys. Rev. Lett. **90**, 120401 (2003).
[8] G. Watanabe, G. Baym and C. J. Pethick, cond-mat/0403470.
[9] G. Baym and C. J. Pethick, cond-mat/0308325.
[10] D. E. Sheehy and L. Radzihovsky, cond-mat/0402637.
[11] N. R. Cooper, N. K. Wilkin, and J. M. F. Gunn, Phys. Rev. Lett. **87**, 120405 (2001).
[12] J. Sinova, C.B. Hanna, and A.H. MacDonald, Phys. Rev. Lett. **89**, 030403 (2002).
[13] A. A. Abrikosov, Zh. Eks. Teor. Fiz. **32**, 1442 (1957) [Sov. Phys. JETP **5**, 1174 (1957)]; W. H. Kleiner, L. M. Roth, and S. H. Autler Phys. Rev. **133**, A1226 (1964).
[14] See *e.g.* N. Read, Phys. Rev. B **58**, 16262 (1998).
[15] N. Read and N. R. Cooper, Phys Rev A **68**, 035601 (2003).
[16] C. B. Hanna, A. J. Sup, J. C. Diaz-Velez, J. Sinova and A. H. MacDonald, APS March Meeting 2004, P28.002.